IJME

Int. J. of Applied Mechanics and Engineering, 2025, vol.30, No.3, pp.42-56
DOI: 10.59441/ijame/205461

SPRINGBACK PREDICTION OF SHEET METAL HYDROFORMING USING FINITE ELEMENT ANALYSIS AND ARTIFICIAL NEURAL NETWORKS

Y. Fartouh[1*], M. Bouzaffour[1] and M. Nassraoui[2]
[1]Génie Mécanique, ENSEM, Hassan II University, B.P 8118 Oasis, Casablanca, MOROCCO.
LMPGI, Higher School of Technology of Casablanca, ESTC, Hassan II University, B.P 8112 Oasis, Casablanca, MOROCCO.
[2]Génie Mécanique, LMPGI, Ecole Supérieure de Technologie de Casablanca, ESTC, Université Hassan II, BP 8112 Oasis, Casablanca, MOROCCO.
E-mail: yassine.fartouh-etu@etu.univh2c.ma

The objective of this paper is to develop a method for the rapid estimating springback in the hydroforming process of circular sheets. First, the springback behavior has been studied with using finite element simulations for various configurations such as sheet thickness, sheet diameter, and deformation pressure. The results obtained shows an excellent correlation with the experimental data. Next, the springback of circular sheets in the setting of hydroforming has been predicted using the artificial neural networks (ANN) approach. Statistical measures, specifically the mean square error (MSE) and the coefficient (R^2) are implemented for evaluating this approach. The results reveal that artificial neural networks provide an accurate, high-performance model for predicting the springback of circular sheets.

Key words: springback, hydroforming, artificial neural networks, machine learning, finite element simulation.

1. Introduction

The hydroforming process is widely utilized in various industrial sectors, especially in the automotive and aerospace industries, which necessitates that sheet metal components should have a specific set of geometric characteristics and mechanical properties [1-2]. This process, particularly in its deep hydrodynamic drawing (HDD) variant, enables sheet metal to be shaped using high fluid pressure. Hence, replacing the conventional punch to ensure precise, homogeneous shaping. A standard sheet metal hydroforming operation is illustrated in Fig.1. The blank metal is placed in the die and held in position by the blank holder before it is deformed under the action of fluid pressure. This pressure generally ranges between *70* and *700 bar* (low pressure) and can reach between *1.400* and *4.800 bar* (high pressure) in exceptional cases, particularly for the manufacture of complex, high-precision parts [3]. This technology also reduces the effect of friction between the blank and the rigid tools used in conventional processes (e.g. the punch) [2]. The growing adoption of this technology in the automotive industry stems from the need to design lighter vehicles in order to reduce energy consumption and pollutant emissions, while guaranteeing optimum mechanical performance (e.g. impact resistance, maximum stress, fatigue, etc.) [1, 2, 4-7]. However, this requirement calls for the use of higher-strength materials, leading to a springback phenomenon. This is the tendency that the sheet to return to its original shape after the hydroforming operation. It is considered as one of the issues found hugely in hydroforming process and more particularly within the automotive industry, it is crucial to correctly predict the springback in order to achieve the desired shape. Without the required shape, assembly of parts becomes extremely difficult and time-consuming. This also results in an increase in the time required for the assembly process [8].

* To whom correspondence should be addressed

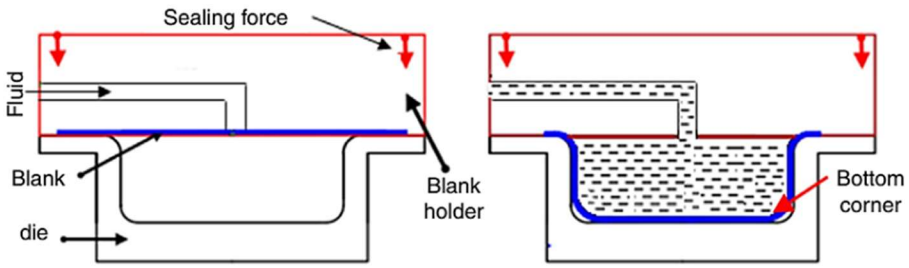

Fig.1. Principle of the hydroforming process [3]

Many approaches to sheet metal forming and springback prediction have been taken by different researchers incorporating various materials and using different modeling and analysis methods. For example, Jiang *et al.* [9] have studied the springback of 5A02 aluminum alloy during hydroforming. They have used theoretical analysis and numerical finite element simulations. They have illustated that hydraulic pressures (*1* to *30 MPa*) and loading paths have a significant influence on springback. This influence varies depending on loading conditions and applied pressures. Su *et al.* [10] have studied the hydroforming of 316L stainless steel bipolar plates using an experimentally validated FEM model. They have analyzed the influence of forming pressure and grain size on springback. The results show a non-linear variation of springback with pressure, and an increase in grain size reduces springback, reaching a maximum of *3.1* μm for a grain size of *60.7* μm. Sun and Lang [11] have obtained a formulation of springback as a function of hydraulic fluid pressure during sheet bending and stretching. Using these relationships, they have shown that when the fluid pressure (deformation load) is higher, the tensile capacity becomes greater, which reduces the springback. In addition, they have analyzed and optimized the hydroforming process for aluminum alloy engine covers, and the optimal process parameters that can reduce the forming steps. They found that part quality could be improved by increasing the pressure applied. Çelik *et al.* [12] have analyzed the influence of radius and angle of curvature, as well as thickness and material type on springback during diaphragm sheet forming. Experiments were carried out with thicknesses ranging from *0.813* to *2 mm*, and results were compared using factorial designs and ANOVA analysis. The study highlights the crucial role of these parameters in mold design, which enables better compensation of springback and optimization of forming quality. Hiseeb and Khleif [13] have carried out an experimental study. The latter has shown that the springback of low-carbon steel parts (1008-AISI) decreases significantly when the fluid pressure and holding time increase. To predict the final geometry of aluminum alloy parts. Churiaque *et al.* [14] have implemented the finite element method using the PAM-STAMP software and some insightful experiments. They have shown that finite element analysis is a very useful method for estimating the springback of hydroformed parts. They have drawn a conclusion that material characterization is an essential step to obtain reliable springback predictions. Lam *et al.* [15] have employed experimental testing and finite element method (FEM) simulation to study the springback of aluminum plates with thicknesses ranging from *3* to *8 mm* during creep forming. In addition, they have examined the influence of initial distortion and residual constraints on the prediction of springback. Fartouh *et al.* [16] have characterized springback during the hydroforming of circular blank using finite element analysis. Later, they have examined how different material factors can affect the springback of hydroformed parts and concluded that these parameters have a significant impact on springback. Nassraoui and Radi [17] have shown that numerical tools combining the finite element method and optimization techniques, play an essential role in controlling, improving and optimizing forming processes in order to minimize the rate of defective parts. Śloderbach [18] demonstrated that the height of spherical shells formed by hydraulic bulging is influenced by stability conditions and key material properties, including hardening behavior and anisotropy. Their work evaluates sheet metal drawability by identifying acceptable plastic strains and associated shell heights under selected instability scenarios.

The use of artificial neural networks (ANN) combined with the finite element method (FEM) is an approach commonly employed in conventional forming processes such as stamping and bending. Several

studies that take into account the variability of process parameters and material properties have been carried out to model and predict the springback phenomenon [19-21].

To fill in the lacuma in this line of research, this work proposes a neural network model for the prediction of springback in sheet hydroforming processes. A numerical finite element simulation model of circular sheet hydroforming has been carefully prepared and validated using experimental tests (bulge test) in order to generate training data for artificial neural networks (ANN). This study analyzes the parameters that influence the springback of steel S235 such as fluid pressure, blank diameter and blank thickness.

2. Methodology

2.1. Finite element simulation model

The researcher has employed the finite element method analysis to simulate the hydroforming and springback of S235 steel sheets using ABAQUS software. The hydroforming simulations have been conducted in two steps. The first step consists of simulating the hydroforming operation of the sheet using an explicit calculation, while the second step consists of simulating the springback after removing the load. The finite element model and the applied boundary conditions (the clamped die and the end of the fixed blank) are shown in Fig.2 (a) and (b). The S4R shell element is implemented to discretize the blank with *7717* elements. The rigid analytical element is used to discretize the die (The die is shown here, although it is a rigid body, in order to apply the contact condition between it and the blank metal). A mesh sensitivity analysis was performed to obtain a sufficient mesh density to ensure accurate results. Figure 2 (c) shows mesh sensitivity analysis: Von Mises stress vs. element size. The results of the distribution of sheet displacements before and after springback illustrated in Fig.3.

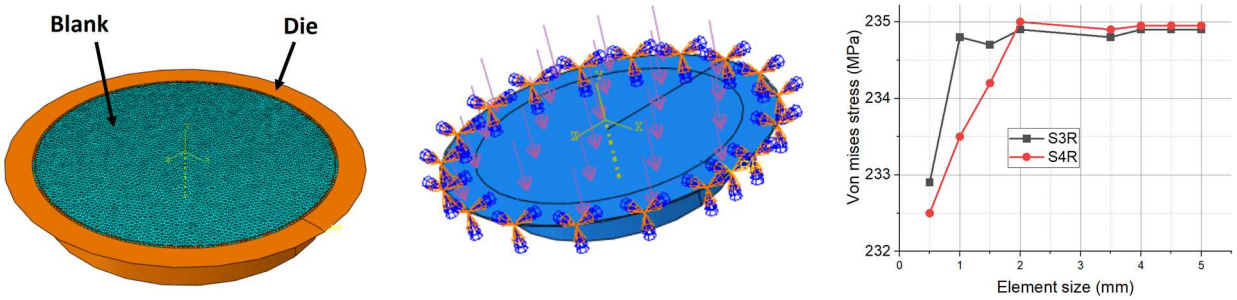

(a) (b) (c)

Fig.2. (a): FE model of sheet hydroforming, (b): boundary conditions and (c): mesh sensitivity.

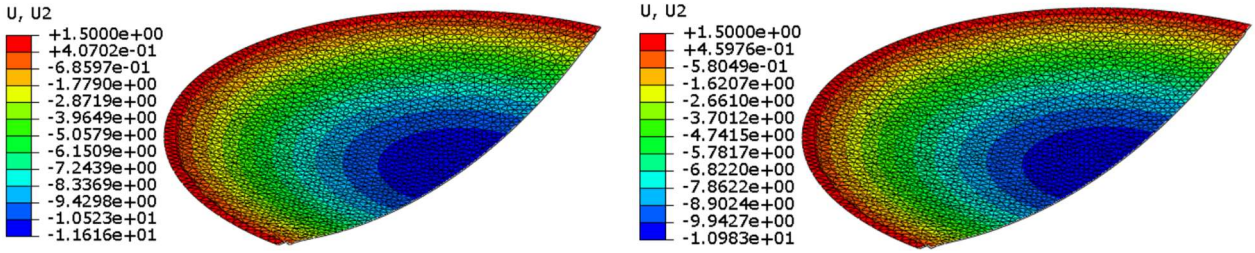

(a) (b)

Fig.3. (a): Displacements before springback and (b): displacements after springback.

The Coulomb friction law model is applied to define the tangential behavior between the die and the blank. A surface-to-surface contact type with a friction coefficient of $\delta = 0.5$ is used for the lubricated steel/steel contact and similar the study [22]. The experimental stress-strain data obtained from the tensile testing was used as input to the ABAQUS model [23]-[24]. The material properties of the S235 raw sheet, obtained from a tensile test, are shown in Tab.1. In addition, the yield strength varies with plastic deformation according to the hardening law. The isotropic hardening law of (Swift, 1952) is represented by Eq.(2.1) [25].

$$\overline{\sigma} = k\left(\varepsilon_0 + \overline{\varepsilon}\right)^n. \tag{2.1}$$

Different simulations of the hydroforming and springback have been realized by modifying the various process parameters (dimensions of the initial part (sheet), the die and the pressure). The thickness *T* is varied from *1 mm* to *3 mm*, the dimensions of the sheet diameter *D* are *120 mm*, *160 mm*, and *198 mm* and for the pressure *P* is varied from *1 MPa* to *2 MPa*.

Table 1. Elastic properties of S235 [23-24].

Parameter	Value
density	*7850 kg/m^3*
yield strength	*235 MPa*
Poisson's ratio	*0.33*
Young's modulus	*21000 MPa*
hardening coefficient	*572.85 MPa*
exponent of hardening	*0.145*

2.2. Experimental procedure

The experimental hydroforming tests have been conducted in the materials science laboratory in the school where the researcher works. Figure 4 shows the experimental equipment for hydroforming circular blank, the die assembly, blank holder and clamping system adding to that an oil evacuation system. The pressure generation system is a hydraulic unit with a capacity of *150 bar*. This system also includes:

- displacement sensor and pressure sensor with data readout,
- data acquisition system,
- computer equipped with data acquisition and processing software,
- cables, accessories and sensor supports etc.

The experimental tests had been executed as soon as the various parameters (displacement and pressure sensors) had been adjusted and checked in the condition of no load. The geometric characteristics of the hydroformed blank have been presented in Tab.2.

Table 2. Experimental validation plan.

Test N°	Blank diameter (*mm*)	Blank thickness (*mm*)
Test 1	*198*	*3*
Test 2	*120*	*2*
Test 3	*120*	*1*
Test 4	*198*	*1*

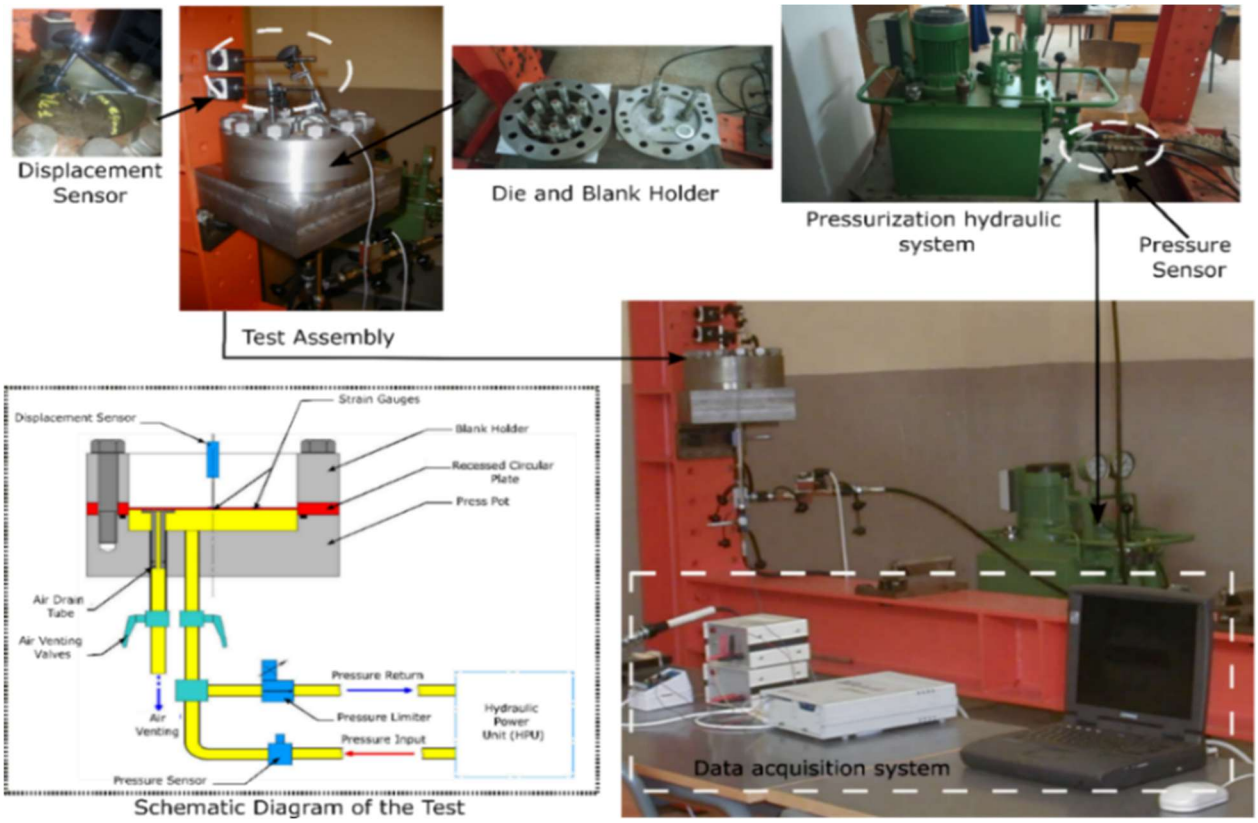

Fig.4. Experimental equipment for hydroforming of circular blank.

2.3. Methodology of machine learning: artificial neural networks

To estimate springback in the hydroforming process of circular sheets, we have employed a machine learning-based strategy. The inputs of the model for each sheet deformation scenario are diameter, thickness, deformation pressure and finite element simulation (FEM) results. Figure 5 illustrates the basic structure of this approach.

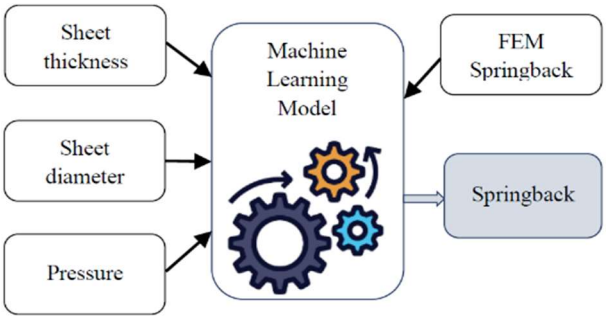

Fig.5. Machine learning diagram.

The development of artificial neural networks as a new discipline in applied computer science has made it possible to solve a number of problems encountered in modelling and optimising various manufacturing processes. They have demonstrated excellent success in modelling complex interactions (both linear and non-linear). This technique is particularly useful for simulating complex problems using physical and mathematical models, thanks to its learning capacity based on practical cases. Among the tools of this

technique are artificial neural networks, which draw on both mathematical theories of learning, information processing and control and human biological neural systems.

The input-receiving layer that sends it to the hidden layer - these used for learning ANN - is named the input layer $\{X_1, X_2, X_3, ... X_n\}$. The neuron receives the weighted values $\{W_1, W_2$ and $W_3 .... W_n\}$ and uses a threshold function, such as the sigmoid function, to modify them. Responses from the hidden layer are received by the output layer, which generates an equivalent result. Figure 6 illustrate the basic structure of an artificial neuron.

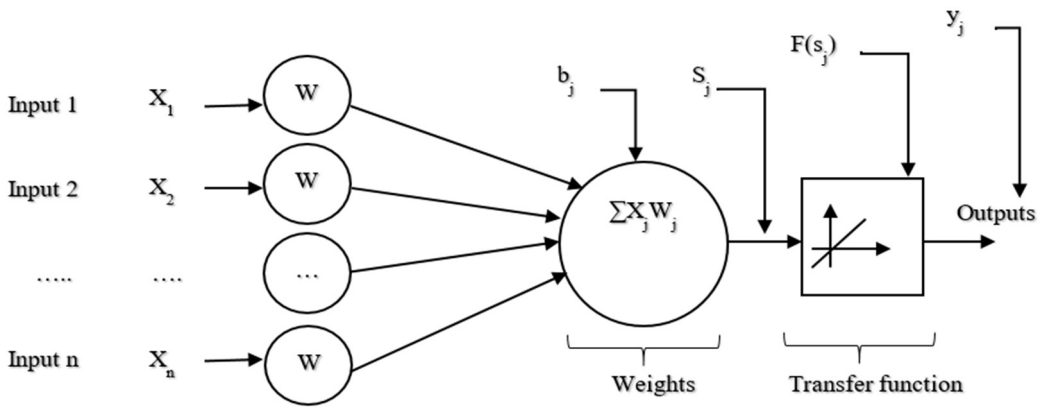

Fig.6. Basic structure of an artificial neuron.

The following Eq.(2.2) represents the intermediate output for each neuron:

$$S_i = \sum_{j=1}^{p} X_j W_{ij} + b_j. \tag{2.2}$$

- p : the number of entries,
- X_j : denotes the value transmitted,
- W_{ij} : the weight stored between the i and j neurons,
- b_j : refers to the bias.

The following Eq.(2.3) represents the overall output of all the neurons:

$$y_i = f(S_i). \tag{2.3}$$

f : the function of activation.

The Levenberg-Marquardt (LM) algorithm has been used to train the network. This algorithm is specifically designed to minimize the sum of squared errors. Figure 7 shows the main steps of the learning process.

Equation (2.4) can be used to update the weights and biases in each neuron:

$$W_{ij}^{z+1} = W_{ij}^{z} + \Delta W_{ij}^{z+1}. \tag{2.4}$$

Equation (2.5) can be used to calculate the change in weight based on the Levenberg-Marquardt algorithm.

$$\Delta W_{ij}^{z+1} = \left[J^T J + \mu I \right]^{-1} J^T e + \alpha \left(W_{ij}^{z} - W_{ij}^{z-1} \right), \tag{2.5}$$

- z : represented the learning step,
- ΔW_{ij}^{z+1} : it refers to the ± incremental adjustment in the weight,
- J : is a Jacobian matrix constituting the primary derivatives of the network errors as a function of the weight and the biases,
- μ : is the training factor,
- I : the matrix of identity,
- e : the error vector of the network,
- α : momentum term.

Equation (2.6) can be used to calculate the mean square error (MSE)

$$MSE = \frac{1}{p} \sum_{j=1}^{p} \left(T_j - a_j \right)^2 \tag{2.6}$$

where:

- p : represented the number of output and input data,
- a_j : are the outputs derived from the inputs w,
- T_j : are the predicted values.

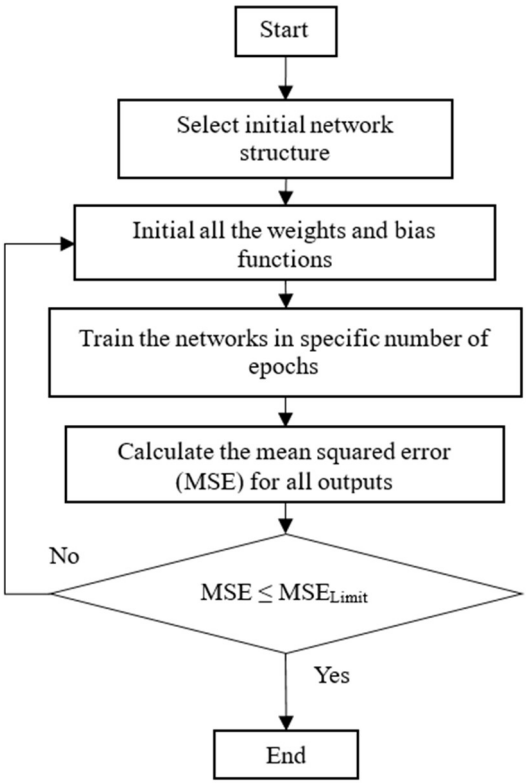

Fig.7. Identification of the optimum ANN architect.

Equation (2.7) can be used to calculate the absolute fraction of variance R^2 :

$$R^2 = 1 - \left(\frac{\sum_{j=1}^{p} (T_j - a_j)^2}{\sum_{j=1}^{p} (a_j)^2} \right). \tag{2.7}$$

Figure 8 illustrates the ANN structure used in this study. It consists of three input layers (thickness *T*, diameter *D* and pressure *P*), one hidden layer and one output (springback). The training data for the neural network are the numerical simulation results. We vary the neurons in each hidden layer to analyze the impact of the number of layers. Different networks were tested for each possible configuration, and the model with the lowest error was selected. Table 3 shows the impact of the hidden layers. The neurons in the hidden layer required to achieve the minimum MSE was set to *20*. The final architecture is thus defined as *3-20-1*.

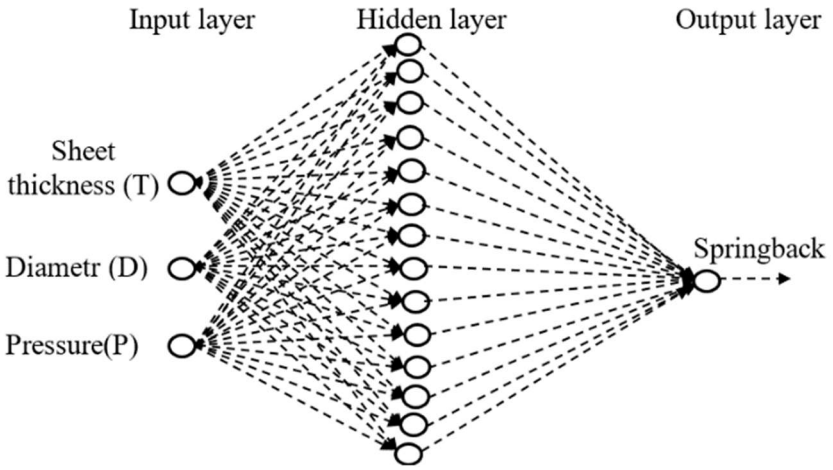

Fig.8. Neural network diagram.

Table 3. MSE and R^2 for each case.

Number of neurons	MSE	R^2
10	*0.0067231*	*0.93113*
12	*0.0056112*	*0.95312*
14	*0.0045631*	*0.96125*
16	*0.00029671*	*0.97255*
18	*0.00013571*	*0.97621*
20	*4.31E-06*	*0.98302*

3. Results and discussion

3.1. Experimental validation test

The experimental tests, we measured the pressure level (*P* in *bar*) and the displacement at the center of the blank (*U* in *mm*) for different blank thicknesses and blank diameters. Figure 9 shows the displacement

at the center of the sheet (in mm) as a function of the pressure of the deformation (in *Bar*). Figure 10 shows the sheet metal before and after deformation.

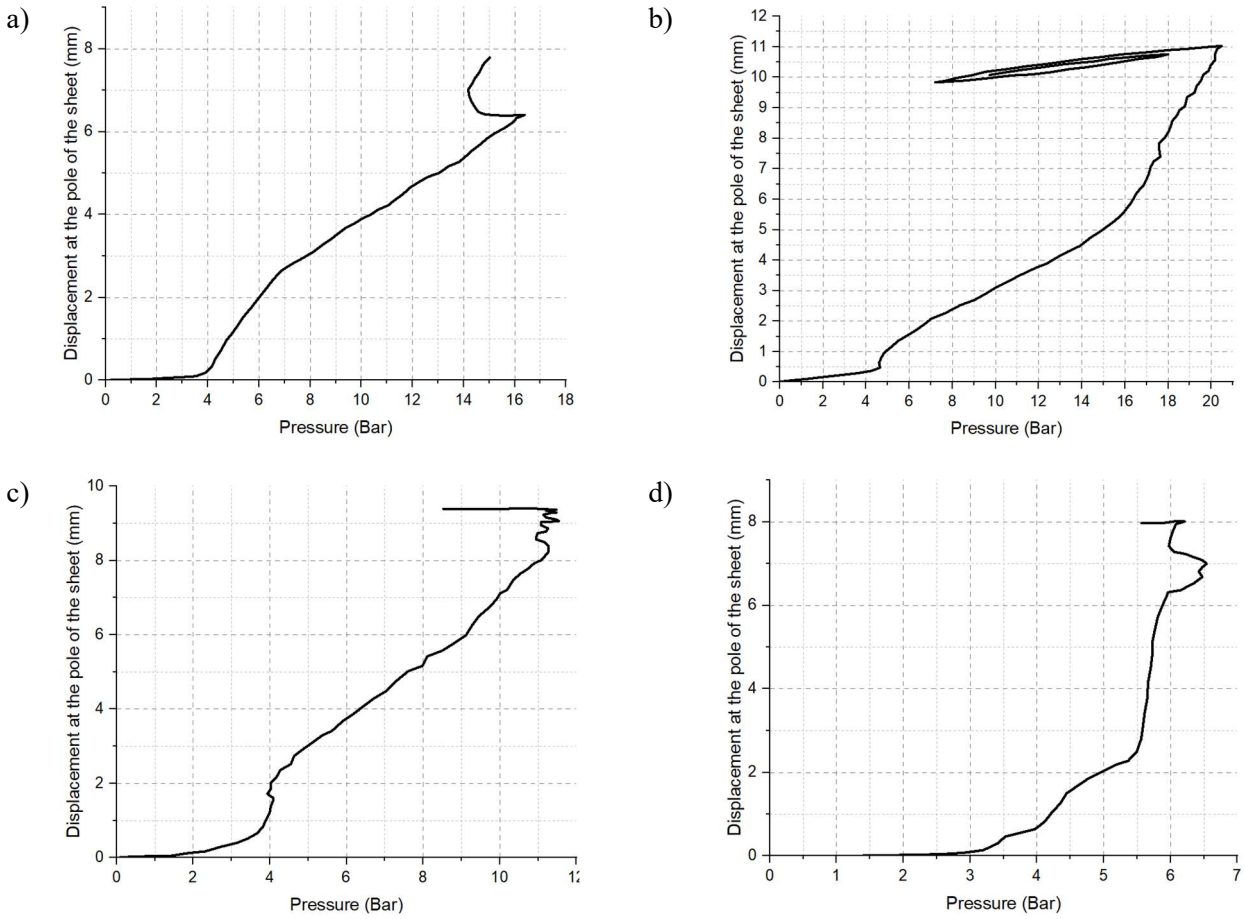

Fig.9. Evolution of the displacement at the center of the sheet (*U*, in *mm*) for the four experimental tests: (a): Test 1, (b): Test 2, (c): Test 3 and (d): Test 4.

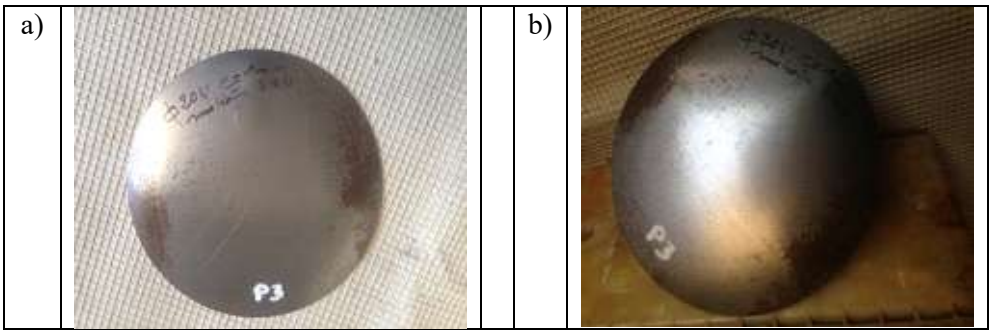

Fig.10. (a): The sheet metal before deformation and (b): The sheet metal after deformation

3.2. Validation of the FEM model

To validate the developed finite element analysis model, a comparison has been made between the experimental results and the numerical results (FEM). Figure 11 shows the distribution of sheet displacements

obtained by FEM. This validation has been realized under the same test conditions (pressure, thickness and diameter), and we have compared the displacement at the center of the blank (U_{EXP} and U_{FEM}). From the Tab.4 and Fig.12, we can deduce that the calculated errors range from *0.28%* to *9.34%.* These discrepancies can be attributed to several factors including the inherent uncertainties in the experimental tests such as measurement errors, variations in material properties, as well as potential differences in loading conditions between the actual tests and the numerical simulation (for instance, the pressure applied to the sheet in the numerical test is assumed to be uniform). Additionally, simplifications and approximations in the numerical model such as the modeling of the steel material or boundary conditions can also contribute to these discrepancies. These errors are generally acceptable for this type of simulation, and the validity of the model is satisfactory. Figure 12 illustrates the error obtained between the experimental results and the numerical results.

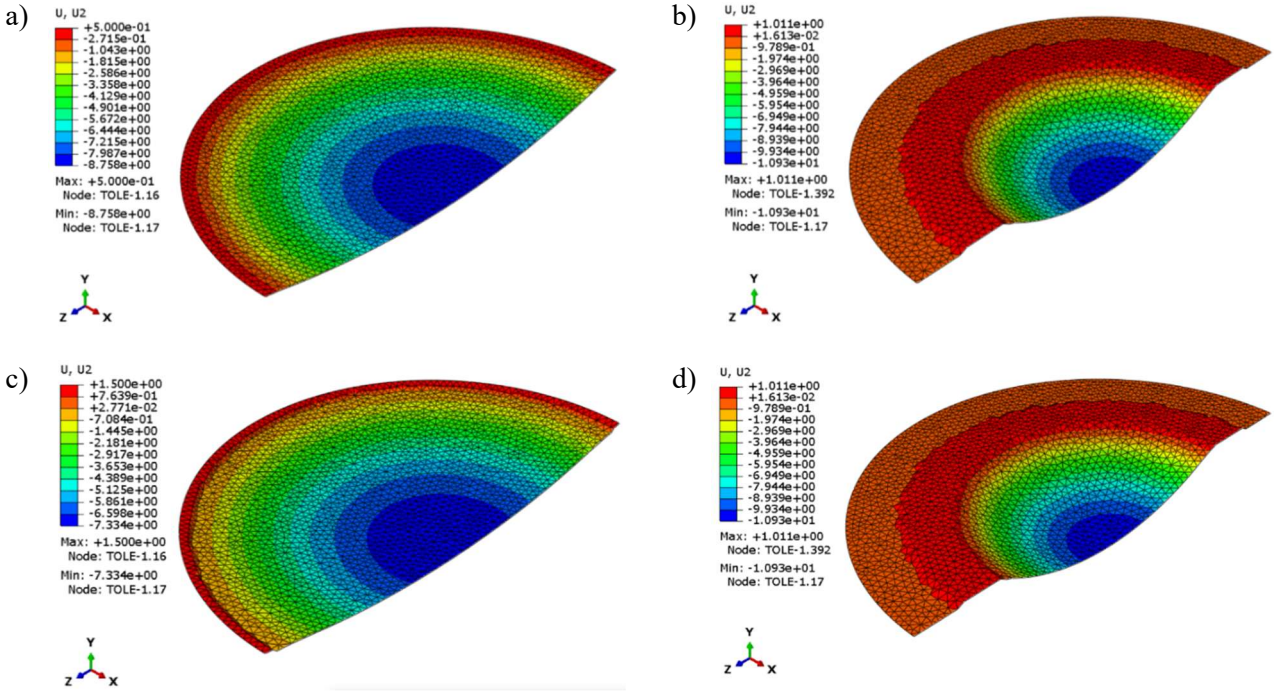

Fig.11. The displacement distribution of the blank obtained using the finite element method (FEM): (a): Test 1, (b): Test 2, (c): Test 3 and (d): Test 4.

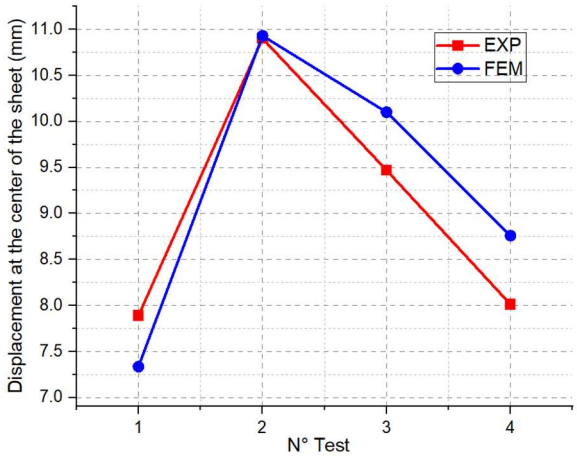

Fig.12. FEM displacement compared to experimental results.

Table 4. Comparison of numerical and experimental displacement results.

Test N°	Diameter *mm*	Thickness *mm*	Pressure *MPa*	U_{Exp} *mm*	U_{FEM} *mm*	Errors %
Test 1	*198*	*3*	*1.639*	*7.89*	*7.334*	*7.05*
Test 2	*120*	*2*	*2.061*	*10.9*	*10.930*	*0.28*
Test 3	*120*	*1*	*1.168*	*9.47*	*10.10*	*6.65*
Test 4	*198*	*1*	*0.611*	*8.01*	*8.758*	*9.34*

3.3. Springback prediction with FEM

This study takes into consideration various thicknesses, sheet diameters and feed pressures. The results obtained from the simulation of springback in circular blank during the hydroforming process are presented in Tab.5 and Fig.13. These results clearly showcase that the amount of springback reduces when there is an increase in forming pressure and sheet diameter. However, it is noticed that springback increases as the sheet thickness increases.

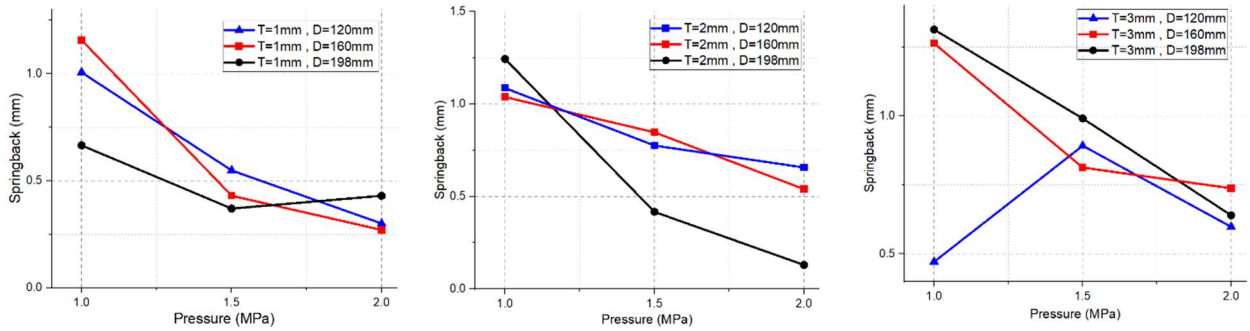

a) b) c)

Fig.13. Effect of the thickness, sheet diameter, and deformation pressure on springback (a): $e = 1mm$, $D = \{120;160;198mm\}$ and $Pressure = \{1;1.5;2MPa\}$, (b): $e = 2mm$, $D = \{120;160;198mm\}$ and $Pressure = \{1;1.5;2MPa\}$ and (c): $e = 2mm$, $D = \{120;160;198mm\}$ and $Pressure = \{1;1.5;2MPa\}$

3.4. Springback prediction with ANN

Figure 14 presents the predictions of springback by neural networks (ANN). The linear regression between all the springback values demonstrates that the points are distributed approximately on a straight line with a gradient approaching *1*.

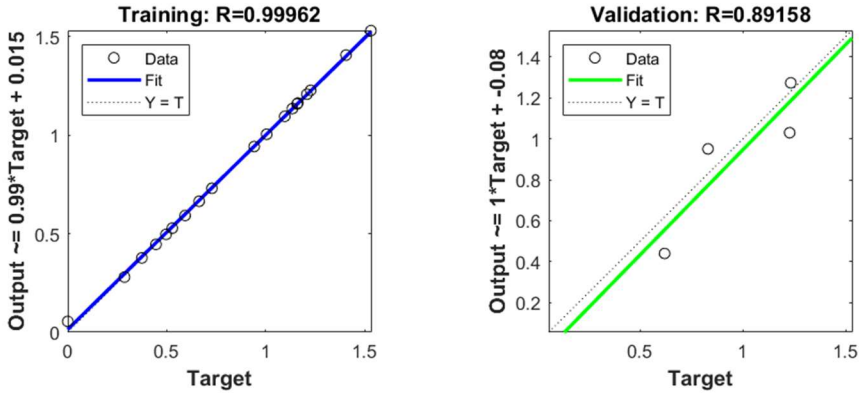

Fig.14. Regression between ANN predicted and FEM Simulation results

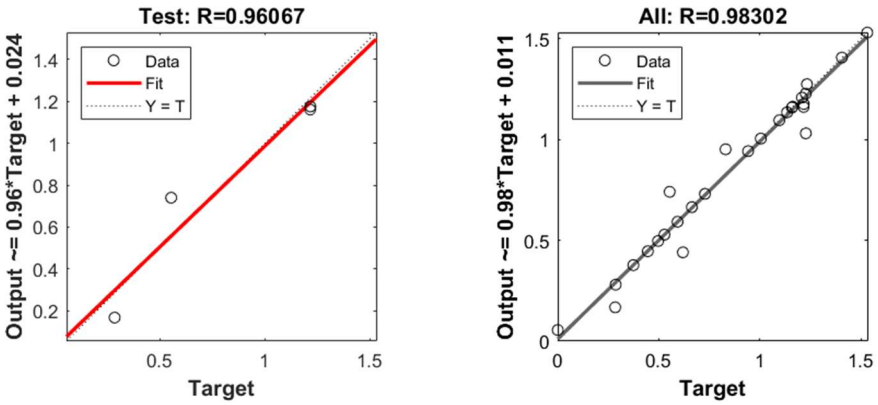

Fig.14. Regression between ANN predicted and FEM Simulation results

Table 5. Comparison of numerical and predicted values of springback.

Test N°	Thickness *mm*	Diameter *mm*	Pressure *MPa*	Springback FEM *mm*	Springback ANN *mm*	Errors %
1	*1*	*120*	*1*	*1.006*	*0.896*	*10.9*
2	*1*	*120*	*1.5*	*0.548*	*0.56*	*2.2*
3	*1*	*120*	*2*	*0.3*	*0.28*	*6.7*
4	*1*	*160*	*1*	*1.157*	*1.037*	*10.4*
5	*1*	*160*	*1.5*	*0.43*	*0.38*	*11.6*
6	*1*	*160*	*2*	*0.27*	*0.24*	*11.1*
7	*1*	*198*	*1*	*0.665*	*0.58*	*12.8*
8	*1*	*198*	*1.5*	*0.37*	*0.34*	*8.1*
9	*1*	*198*	*2*	*0.43*	*0.39*	*9.3*
10	*2*	*120*	*1*	*1.0865*	*0.9765*	*10.1*
11	*2*	*120*	*1.5*	*0.776*	*0.866*	*11.6*
12	*2*	*120*	*2*	*0.657*	*0.597*	*9.1*
13	*2*	*160*	*1*	*1.038*	*1.028*	*1.0*
14	*2*	*160*	*1.5*	*0.847*	*0.947*	*11.8*
15	*2*	*160*	*2*	*0.54*	*0.48*	*11.1*
16	*2*	*198*	*1*	*1.244*	*1.134*	*8.8*
17	*2*	*198*	*1.5*	*0.417*	*0.407*	*2.4*
18	*2*	*198*	*2*	*0.13*	*0.141*	*8.5*
19	*3*	*120*	*1*	*0.4714698*	*0.50147*	*6.4*
20	*3*	*120*	*1.5*	*0.892*	*0.882*	*1.1*
21	*3*	*120*	*2*	*0.598*	*0.52*	*13*
22	*3*	*160*	*1*	*1.26309*	*1.3309*	*5.4*
23	*3*	*160*	*1.5*	*0.813*	*0.903*	*11.1*
24	*3*	*160*	*2*	*0.738*	*0.68*	*7.9*
25	*3*	*198*	*1*	*1.313*	*1.403*	*6.9*
26	*3*	*198*	*1.5*	*0.991*	*0.881*	*11.1*
27	*3*	*198*	*2*	*0.64*	*0.71*	*10.9*

3.5. Discussion

The results obtained with the FEM method for springback prediction shows that forming pressure and blank diameter are the two most influential parameters on the springback of hydroformed sheets. The latter decreases when the forming pressure and sheet diameter increase. However, sheet thickness plays a significant role in this context since the sheet thickness increases when the springback increases. The applied artificial neural networks approach based on the Levenberg-Marquardt algorithm has been adopted as the learning method for multi-layer networks. Different configurations have been tested with the neurons the hidden layer is varying from *10* to *20* (Tab.3). Statistical measures, specifically the mean square error (MSE) and the coefficient (R^2) are used for evaluating this approach. The most convenient results have been obtained which used *20* neurons. ANN prediction of springback has been confirmed with numerical results (FEM). Table 6 and Fig.15 show the numerical and the corresponding predictions of the artificial neural network (ANN) for springback. It can be deduced that the maximum error is *13%.* These results show that the values obtained by the FEM method and those predicted by the ANN model were very close to each other. This discrepancy remains acceptable within the scope of this study and can be regarded as a potential area for improvement for ANN models. Future improvements could include the integration of additional training data and optimization of the neural network structure, which would help reduce the gaps between FEM and ANN results while maintaining the speed of the prediction process.

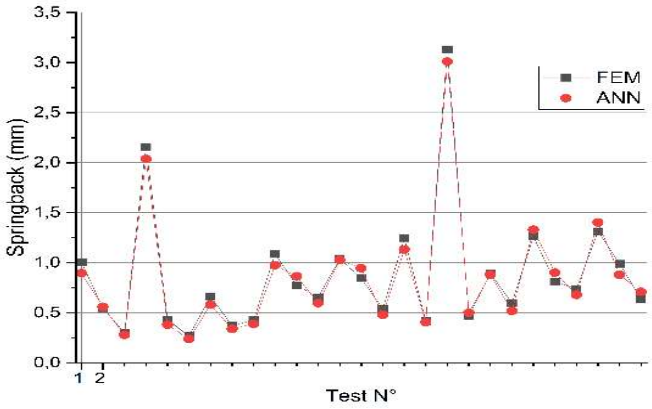

Fig.15. Predicted springback values: ANN vs. FEM.

4. Conclusions

This paper presents experiments and numerical simulations of the hydroforming process of a circular S235 steel sheet. The comparison between the numerical simulations and results from experiments, in terms of displacement at the center of the sheet shows excellent consistency, which makes it possible to validate the numerical analysis carried out using the finite element method (FEM) simulation. The FEM and ANN methods have been used later to predict springback. The springback predicted by the numerical simulations was used as input for the ANN, it was trained using the Levenberg-Marquardt (LM) backpropagation algorithm with *20* neurons and was built on a multilayer forward propagation architecture. A mean square error (MSE) of *4.31E-06* and a coefficient of determination R^2 of *0.98302* were obtained. The results revealed strong agreement between the springback predictions obtained by ANN and those derived from the FEM method. However, our prediction model could be improved in a future studies by using experimental values of springback without relying on numerical simulation (FEM). Integrating these experimental data would allow for better adjustment of the model parameters. Furthermore, increasing the diversity of the training data, as well as optimizing the number of neurons in the hidden layers would help improve the generalization of the ANN model. These improvements would make the model more robust to variations in process conditions and increase its ability to predict results in scenarios not observed in the initial training dataset.

Nomenclature

ANN – artificial neural network
a_i – outputs derived from the inputs
b_j – refers to the bias for the neuron
e – error vector of the network
FEM – finite element analysis
I – matrix of identity
J – jacobian matrix
k – hardening coefficient
MSE – mean square error
n – strain hardening exponent
R^2 – coefficient of determination
s_i – intermediate output for each neuron
T_j – predicted values
U – displacement, *mm*
w_{ij} – the weight stored between the *i* and *j* neurons
X_j – denotes the value transmitted
y_i – the function of activation
Z – represented the learning step,
α – momentum term
Δw_{ij} – it refers to the ± incremental adjustment in the weight
δ – coefficient of friction
$\bar{\varepsilon}$ – equivalent strain
ε_0 – elastic strain
μ – training factor
$\bar{\sigma}$ – equivalent stress, *MPa*

References

[1] Hwang Y.M. and Manabe K.I. (2021): *Latest hydroforming technology of metallic tubes and sheets*.– Metals, vol.11, No.9, pp.1360, doi.org/10.3390/met11091360.

[2] Chinchanikar S., Mulik H., Varude P., Atole S. and Mundada N. (2024): *A review of emerging hydroforming technologies: design considerations, parametric studies, and recent innovations*.– Journal of Engineering and Applied Science, vol.71, No.1, pp.205, doi.org/10.1186/s44147-024-00546-z.

[3] Feyissa F.T. and Kumar D.R. (2019): *Enhancement of drawability of cryorolled AA5083 alloy sheets by hydroforming*.– Journal of Materials Research and Technology, vol.8, No.1, pp.411-423, doi.org/10.1016/j.jmrt.2018.02.012.

[4] Bell C., Corney J., Zuelli N. and Savings D. (2020): *A state of the art review of hydroforming technology*. – International Journal of Material Forming, vol.13, No.5, pp.789-828, doi.org/10.1007/s12289-019-01507-1.

[5] Lihui L., Kangning L., Cai G., Yang X., Guo C. and Bu G. (2014): *A critical review on special forming processes and associated research for lightweight components based on sheet and tube materials*.– Manufacturing Rev., vol.1, pp.9, doi.org/10.1051/mfreview/2014007.

[6] Landgrebe D. and Schieck F. (2015): *Hot gas forming for advanced tubular automobile components: opportunities and challenges*.– Proceedings of the ASME 2015 International Manufacturing Science and Engineering Conference, vol.1, Processing. Charlotte, North Carolina, USA, June 8-12, V001T02A087, doi.org/10.1115/MSEC2015-9204.

[7] Trzepieciński T. (2020): *Forming processes of modern metallic materials*.– Metals, vol.10, No.7, pp.970, doi.org/10.3390/met10070970.

[8] Spišák E., Majerníková J., Mulidrán P. and Hajduk J. (2025): *Springback analysis and prediction of automotive steel sheets used in compression bending*.– Materials, vol.18, No.4, pp.774, doi.org/10.3390/ma18040774.

[9] Jiang P., Lang L. and Alexandrov S. (2020): *Research on springback of 5A02 aluminum alloy considering thickness normal stress in hydroforming*.– In Proceedings of the Third International Conference on Theoretical, Applied and Experimental Mechanics, Springer International Publishing, pp.151-157, doi.org/10.1007/978-3-030-47883-4_26.

[10] Su Z., Xie W., Xu Y., Li C., Xia L., Yang B., Gao M., Song H. and Zhang S. (2024): *Study on springback behavior in hydroforming of micro channels for a metal bipolar plate*.– Materials, vol.17, No.21, pp.5386, doi.org/10.3390/ma17215386.

[11] Sun Z. and Lang L. (2017): *Effect of stress distribution on springback in hydroforming process*.– Int. J. Adv. Manuf. Technol., vol.93, No.5-8, pp.2773-2782, doi.org/10.1007/s00170-017-0670-x.

[12] Çelik Y., Ülke I., Yurdakul M. and Tansel Y. (2024): *A springback minimization study using the experimental design methods for 15-5 PH stainless steel material in the hydroforming process.*– World Journal of Engineering, doi.org/10.1108/WJE-08-2024-0457.

[13] Hiseeb H.A.J. and Khleif A.A. (2024): *Experimental investigations of a springback in hydromechanical deep drawing of low carbon steel 1008 AISI*.– Tikrit Journal of Engineering Sciences, vol.31, No.2, pp.20-27, doi.org/10.25130/tjes.31.2.3.

[14] Churiaque C., Sánchez-Amaya J.M., Caamaño F., Vazquez-Martinez J.M. and Botana J. (2018): *Springback estimation in the hydroforming process of UNS A92024-T3 aluminum alloy by FEM simulations.*– Metals, vol.8, No.6, pp.404, doi.org/10.3390/met8060404.

[15] Lam A.C.L., Shi Z., Lin J. and Huang X. (2015): *Influence of residual stresses and initial distortion on springback prediction of 7B04-T651 aluminum plates in creep-age forming*.– Int. J. Mech. Sci., vol.103, doi.org/10.1016/j.ijmecsci.2015.09.004.

[16] Fartouh Y., Dahbi Y., Nassraoui M. and Otmane B. (2022): *Study of effect of material parameters on springback of hydroformed parts.*– Int. Journal on Technical and Physical Problems of Engineering, vol.14, No.2, pp.360-368.

[17] Nassraoui M. and Radi B. (2016): *Study of optimizing a tube hydroforming*.– 2016 4th IEEE International Colloquium on Information Science and Technology (CiSt), Tangier, Morocco, IEEE, pp.7130-7138, doi.org/10.1109/CIST.2016.7804979.

[18] Śloderbach Z. (2015): *Conditions of stability loss puring the test of hydraulic forming of drawpieces.*– International Journal of Applied Mechanics and Engineering, vol.20, pp.917-938, doi.org/10.1515/ijame-2015-0059.

[19] Spathopoulos S.C. and Stavroulakis G.E. (2020): *Springback prediction in sheet metal forming, based on finite element analysis and artificial neural network approach*.– Applied Mechanics, vol.1, No.2, pp.97-110, doi.org/10.3390/applmech1020007.

[20] Dib M., Ribeiro B. and Prates P. (2018): *Model prediction of defects in sheet metal forming processes*. – In Engineering Applications of Neural Networks, Pimenidis E, Jayne C, editors. Cham: Springer International Publishing, pp.169-180, doi.org/10.1007/978-3-319-98204-5_14.

[21] Dib M., Ribeiro B. and Prates P. (2020): *Single and ensemble classifiers for defect prediction in sheet metal forming under variability.*– Neural. Comput. & Applic., vol.32, No.16, pp.12335-12349, doi.org/10.1007/s00521-019-04651-6.

[22] Nassraoui M. and Radi B. (2020): *An exploratory study of the sheet hydroforming process.*– IncertFia vol.4. No.1, doi.org/10.21494/ISTE.OP.2020.0567.

[23] Nassraoui M., Zakaria E. and Bouchaib R. (2018): *Experimental characterization of hydroforming*.– IncertFia, vol.2, No.1, doi.org/10.21494/ISTE.OP.2018.0255.

[24] Ghazouani N., Toumi M., Aladeb A., Salah W., Tashkandi M. and Becheikh N. (2024): *The characterization of the plastic instability of S235 thin steel sheets by multiple regression and analysis of variance methods*.– Mechanics, vol.30, No.1, pp.5-13, doi.org/10.5755/j02.mech.34036.

[25] Ben Abdessalem M.A. (2011): *Optimization with taking into account of uncertainties in hydroformig process*.– Theses, INSA de Rouen.

Received: February 4, 2025
Revised: May 22, 2025